Opto-Electronic Advances

Supplementary information

May 2025, Vol. 8, No. 5

DOI: 10.29026/oea.2025.240293 CSTR: 32247.14.oea.2025.240293

Spectrally extended line field optical coherence tomography angiography

Si Chen[1,2], Kan Lin[1], Xi Chen[1], Yukun Wang[1,4], Chen Hsin Sun[2,5], Jia Qu[6,7], Xin Ge[1,8], Xiaokun Wang[4] and Linbo Liu[1,3]*

[1]School of Electrical & Electronic Engineering, Nanyang Technological University, Singapore 639798, Singapore; [2]Department of Ophthalmology, Yong Loo Lin School of Medicine, National University of Singapore, Singapore 117597, Singapore; [3]Guangzhou National Laboratory, Guangzhou 510320, China; [4]State Key Laboratory of Applied Optics, Changchun Institute of Optics, Fine Mechanics and Physics, Chinese Academy of Science, Changchun 130033, China; [5]Department of Ophthalmology, National University Hospital, Singapore 119074, Singapore; [6]National Engineering Research Center of Ophthalmology and Optometry, Eye Hospital, Wenzhou Medical University, Wenzhou 325027, China; [7]Oujiang Laboratory, Zhejiang Lab for Regenerative Medicine, Vision and Brain Health, Wenzhou 325101, China; [8]School of Science, Shenzhen Campus of Sun Yat-sen University, Shenzhen 518107, China.

*Correspondence: LB Liu, E-mail: liu_linbo@gzlab.ac.cn

This file includes:

Supplementary information for this paper is available at https://doi.org/10.29026/oea.2025.240293

Section 1: 1310 nm OCT system for skin angiographic imaging

1.1 Detailed system design and construction

We used a superluminescent diode module (IPSDS1313, Inphenix, CA, USA), which provided spectral output from ~1240 nm to ~1360 nm (−6 dB) (Fig. 1). The outputs of the fibre coupler are guide by two optical circulators (PIBCIR-1214-12-L-10-FA, FOPTO, Shenzhen, China) to the sample arm and reference arm, respectively. The light back reflected from the reference arm and back-scattered from the sample arm are combined using a 95:5 fibre coupler (WP3105202A120511, AC Photonics, CA, USA).

In the sample arm of the point scanning configuration, the sample beam is firstly collimated by an achromatic lens L1 with a focal length of 10 mm (AC050-010-C, Thorlabs Inc., USA) before reflected by a mirror (RM) and a pair of galvanometer scanners, and focused by an objective lens L2 having a focal length of 50 mm (AC254-050-C, Thorlabs Inc, USA). In the SELF configuration, the mirror (RM) is replaced by a set of 3 identical prisms (N-SF11, PS872-C, Thorlabs Inc.). The prism is with anti-reflection coating so that one-way transmission efficiency of three prisms was measured to be 94%. The mirrors of the galvanometer scanners can support beam diameter of 5 mm. In SELF configuration, the beam diameter is ~2.6 mm at 1% power level on the scanner mirrors. The distance between the prisms and the Y scanning mirror is less than 60 mm, with the maximum diverging angle of 5.03 mrad between the principal rays of the polychromatic beam, the beam displacement is less than 0.30 mm. The prism dispersion expands the spot size to 2.90 mm.

The spectrometer is comprised of a collimating lens L5 (AC254-035-C, Thorlabs Inc., USA), a transmission grating (PING-sample-106, Ibsen Photonics, Denmark), a home-made multi-element camera lens and a line scan camera (LDH2, Sensors Unlimited, USA). The camera pixel size is 25 μm by 500 μm (width by height) and we use all 1024 pixels. The detected FWHM spectral bandwidth is 90 nm. The total spectrometer efficiency is measured to be 0.61, including the quantum efficiency of the camera. The spectral resolution is 0.148 nm, resulting in a total ranging depth of 2.89 mm in air. The axial resolution is measured to be 10.07 μm in air and the transverse resolution is calculated to be 27.06 μm. The measured 6 dB ranging depth is 1.6 mm in air and the sensitivity roll-off over depth is ~3.75 dB/mm.

With the optical power incident on the sample being 4.74 mW, the system sensitivity measured at ~150 μm from DC is 108.52 dB, 102.56 dB, and 98.58 dB at the A-line rate of 22000 Hz, 50000 Hz, and 80384 Hz, respectively using a partial reflector (−33.65 dB). The theoretical sensitivity (S) is given by[S1, S2]:

$$S = 10 \times \log\left(\frac{\sum N_s \times N_{\text{ref}}}{N_{\text{shot}}^2 + N_{\text{excess}}^2 + N_{\text{receiver}}^2}\right) , \tag{S1}$$

where $\sum N_S$ and N_{ref} denote the electrons over the entire CCD array generated by sample arm light and electrons per pixel given by the reference arm light returning from a perfect reflector (100% reflectivity), respectively, N_{shot}^2 , N_{excess}^2, and N_{receiver}^2 represent electrons from shot noise, excess noise and receiver noise (electrical noise), respectively[S1,S2]. OCT maximum SNR (sensitivity) was obtained with $N_{\text{receiver}} = N_{\text{excess}} = 3346$. Since $N_{\text{shot}} = 2259$, 1828, and 1614 at 22000 Hz, 50000 Hz and 80384 Hz respectively, the system is receiver noise limited.

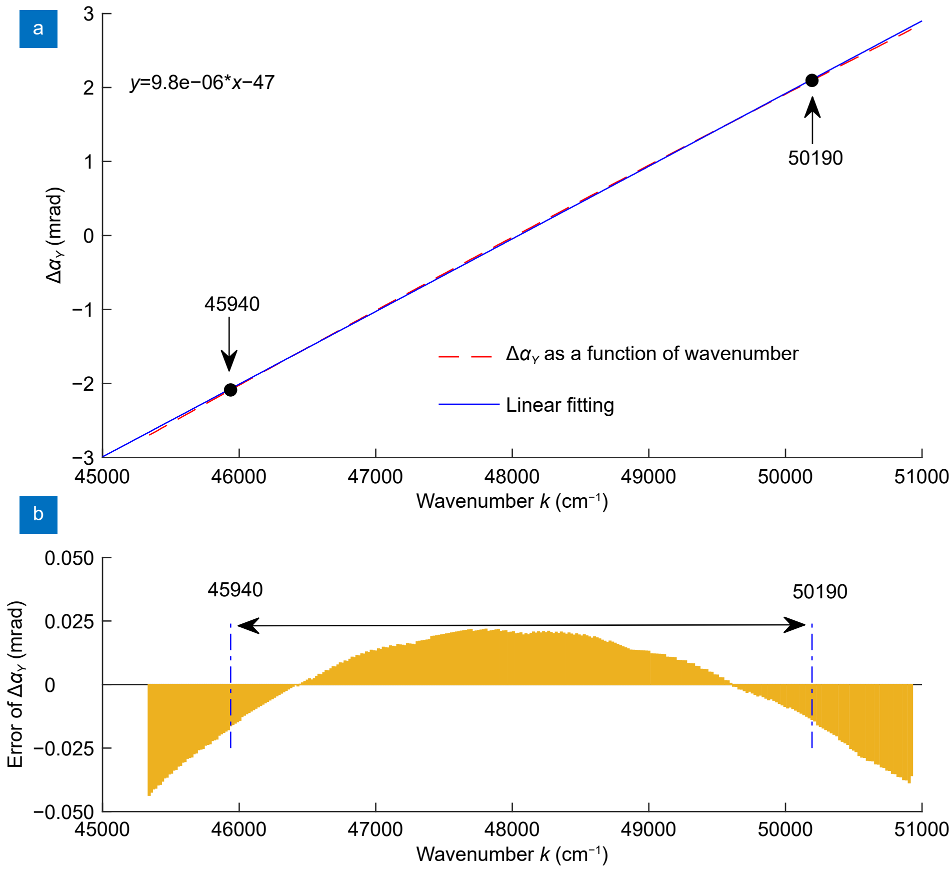

Fig. S1 | (**a**) field angle along line field at *Y*-axis ($\Delta\alpha_Y$) as a function of wave number (K) (red dash line). Blue solid line is the linear fitting. The center wave number of the 1st and 16th spectral band are 4594 cm^{-1} and 5019 cm^{-1}, respectively. (**b**) The corresponding linear error of $\Delta\alpha_Y$ is <0.0217 mrad within the range from 45940 cm^{-1} to 50190 cm^{-1}, corresponding to <1.0855 μm in the focal plane of the objective lens.

1.2 Linear relation between *Y* coordinate and the wavenumber

We start with the assumption that the transverse distance is a linear function of wavenumber. We know that wavelength range of the spectrometer is from 1233.8 nm to 1386.2 nm from the optical design in Zemax. We then conducted a simulation using optical parameters of the prism to calculate the field angle at the objective lens $\Delta\alpha_Y$ as a function of wavenumber. The linear error between the field angle and the wavenumber is confirmed to be <0.0217 mrad between the center of the 1st spectral band (~50190 cm^{-1}) and the center of the 16th spectral band (~45940 cm^{-1}), which corresponds to <1.0855 μm in the focal plane of the objective lens (Fig. S1). This simulation result confirms that nonlinear error associated with the above-mentioned linear assumption is negligible.

The Hamming window length in terms of pixels in wavenumber space is determined in the edge scan experiment using USAF 1951 resolution chart. To do so, we firstly multiply the interference fringes in the wavenumber domain with two narrow Hamming windows far apart from each other, which gives 2 partial-spectrum 3D images. By measuring the *Y* position difference of the same edge between the two partial spectrum *en face* projections we can obtain the slope of the linear relation in terms of transverse coordinate (mm) over wavenumber in (cm^{-1}): ~4.51×10^{-5}. With this slope, we determine that the spacing between the centers of two adjacent Hamming window is 52 pixels in wave number space which corresponds to ~284.12 cm^{-1} or 12.8 μm in *Y*-axis (Fig. S2). The total length of Hamming window can be calculated in the same way, which is 263 pixels, corresponding to ~1,437 cm^{-1} or 64.74 μm in wavenumber space along *Y*-axis (Fig. S2).

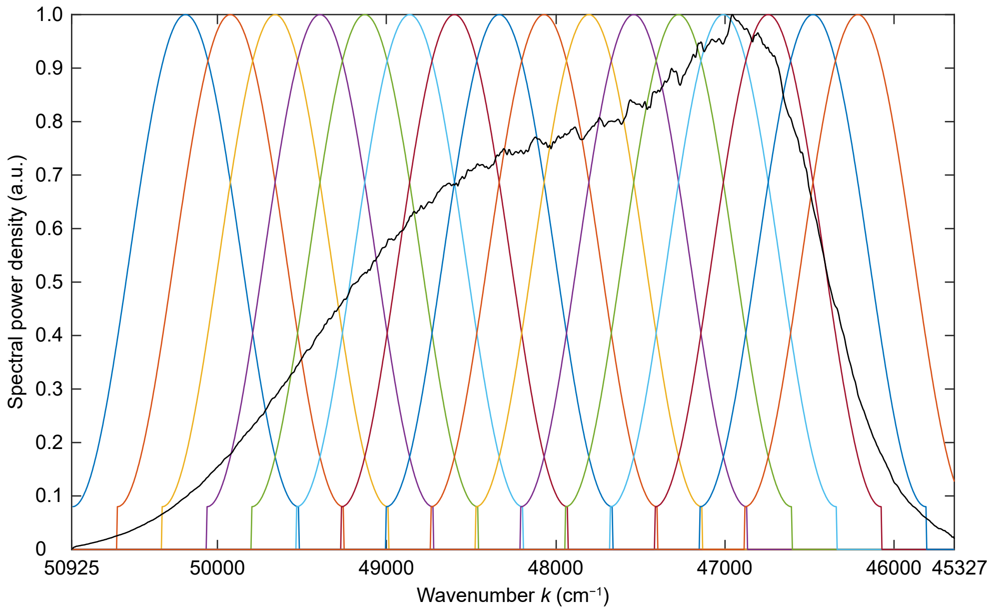

Fig. S2 | Source spectrum detected by the OCT spectrometer in *k*-space overlapped with *M* =16 Hamming filters.

1.3 Spectral window filtering on the transverse PSF

To numerically evaluate the effect of the spectral window, which is Hamming filtering in this study, on the transverse PSF, we simulated the convolution between the monochromatic PSF and the Hamming window in the spatial domain along *Y*-axis (Fig. S3). Please note that the Hamming function can be translated from wavenumber domain to the spatial domain along *Y* axis based on the above-mentioned linear assumption. In Fig. S3, all the functions are in arbitrary unit because in this simulation we are interested in the ratio between the widths of monochromatic PSF and polychromatic PSF. The monochromatic PSF in the transverse plane was modeled as a Gaussian function. The FWHM of the monochromatic PSF is 24.1 μm from our resolution characterization results, and FWHM of Hamming window is 33.94 μm from our edge scan experiment using resolution target. The result of the simulation demonstrates that the polychromatic PSF is 52% broader in *Y*-axis than that of the monochromatic PSF (Fig. S3).

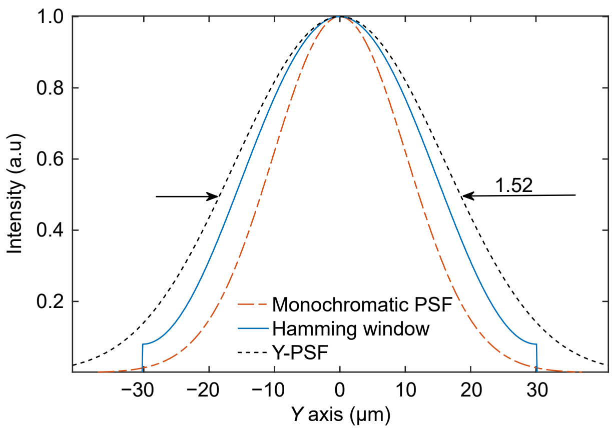

Fig. S3 | Broadening of transverse point-spread function. Transverse point-spread function (PSF) along *Y*-axis (*Y*-PSF) as the result of convolution between the Hamming window and monochromatic PSF.

1.4 Maximum permissible exposure of line field on skin

Following the literature[S3], the relevant 'most restrictive' evaluation angular subtense is the one with the maximum ratio of partial power to evaluation angular subtense. The partial power is the total optical power contained in the evaluation angular subtense. The intensity profile of the line field was measured by scanning a fiber tip (SMF-28e) along *Y*-axis in the focal plane of the objective lens and record the optical power coupled into the fiber. The angular subtense along *X*-axis takes 1.5 mrad[S4]. Since it is a line illumination along *Y* axis, the ratio of partial power/ evaluation angular subtense

$$\frac{P}{\delta} = 2P/(\alpha_Y + 1.5\ \mathrm{mrad}). \tag{1}$$

According to the Eq. (1), the angular subtense in *Y*-axis (α_Y) obtained using 'Most restrictive ratio' analysis is 3.176 mrad (Fig. S4(b)). The corresponding wavelength range is approximately from 1251.9 nm to 1367.7 nm, covering a transverse distance of 159 μm at the centre of the line field (Fig. S4(a)). The extended source correction factor C_E is (3.176 +1.5 mrad) / (1.5+1.5 mrad) = 1.5587 where the angular subtense along both *X*-axis and *Y*-axis is 1.5 mrad for the point source. Note that power limit calculated using C_E applies only to the partial power within the angular subtense δ, instead of the total power. As shown inFig. S4, there are 20.11% of total power that is outside the angular subtense δ.

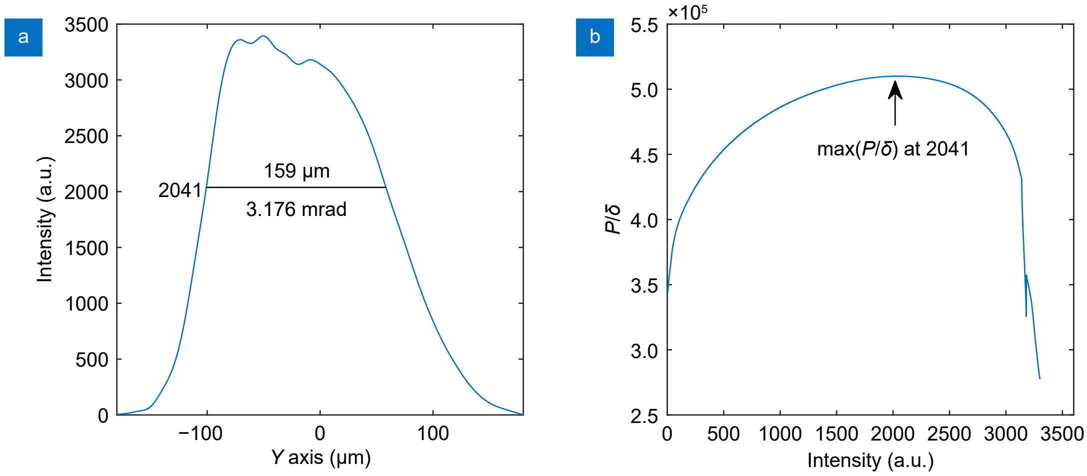

Fig. S4 | Maximum permissible exposure characterization for 1300 nm system. (**a**) Intensity profile of focus along *Y*-axis. (**b**) Ratio between partial power (*P*) within window width (δ) for 'Most restrictive ratio' method. The window width is 159 μm (3.176 mrad) when the ratio reaches the maximum.

For skin imaging with point-scanning configuration running at 50000 Hz A-scan rates, the optical power incident on the sample is 4.74 mW. The corresponding power for the SELF configuration is calculated as (4.74 mW × C_E) / (1−0.2011) = 9.25 mW and ~9.10 mW was used for the skin imaging with SELF configuration in this study.

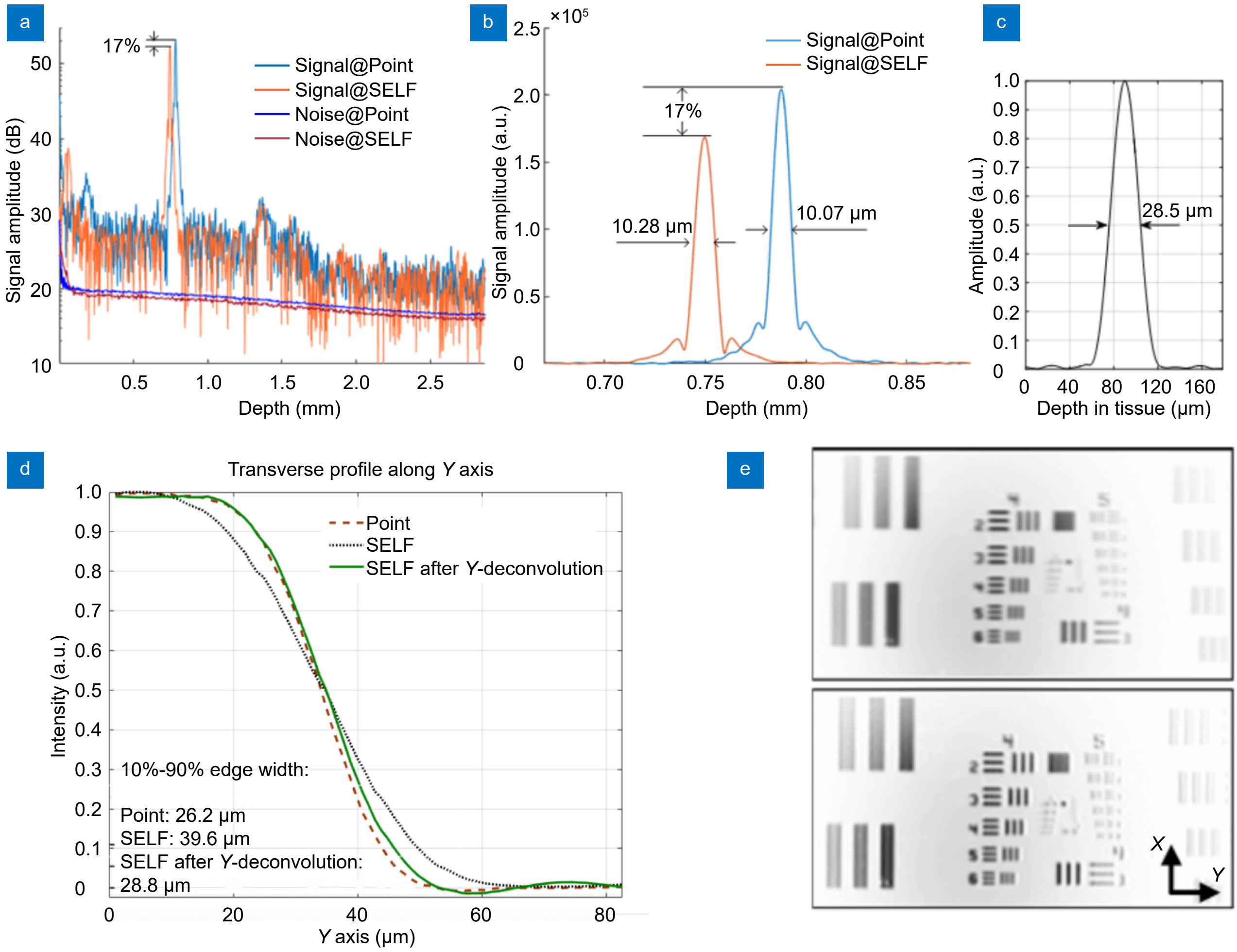

Fig. S5 | Sensitivity and spatial resolution characterization of the 1300 nm system. (**a**) Axial profiles and noise floor of full-spectrum fringe data in log scale. (**b**) Axial profiles of full-spectrum fringe data in linear scale with FWHM axial resolution being 10.07 μm and 10.28 μm, respectively. (**c**) Normalized axial profile of a partial-spectrum fringe data (8th partial spectrum). (**d**) Transverse profile along *Y*-axis of a quasi-monochromatic beam (orange dash line), beam of the 8th partial spectral band before (dark dot line) and after *Y*-deconvolution (green solid line). (**e**) *En face* images of USAF 1951 resolution chart obtained using the partial-spectrum of the 8th spectral band before (upper panel) and after *Y*-deconvolution (lower panel).

Section 2: 850 nm OCT system for retina angiographic imaging

2.1 System construction and calibration

A superluminescent diode source with a central wavelength of 850 nm and spectral bandwidth of ~175 nm (165 nm at −3 dB) ranging from 755 nm to 930 nm was used (cBLMD-T-850-HP) to develop the system for retinal imaging (Fig. S6). In retina imaging except for Fig. 3(g–j), we utilize only a portion of the spectral bandwidth, approximately 90 nm (−3 dB), with the first diode channel of the light source switched off and a short-pass filter in the sample arm (TSP01-887-25×36, semrock). The light source is connected to a 75:25 fibre coupler (TW850R3A2, Thorlabs Inc, USA) and the outputs of the fibre coupler guide the light beams to the sample arm and reference arm, respectively. The light back reflected from the two arms is combined and is directed to the spectrometer. In the sample arm, the beam of the point scanning configuration is collimated by an achromatic lens L1 (AC050-008-B, Thorlabs Inc., USA) and reflected to *X*-*Y* galvanometer scanners (ScannerMAX Saturn) through a reflective mirror (RM) before directed to a telescope system. The beam of the point scanning configuration is collimated by the same lens L1 and passes through a prism with 30° apex angle (N-SF11) before it is directed to the *X*-*Y* scanner. A manual translation stage is used to switch the scanning mode between the point configuration and the SELF configuration. The telescope system contains two sets of 200 mm

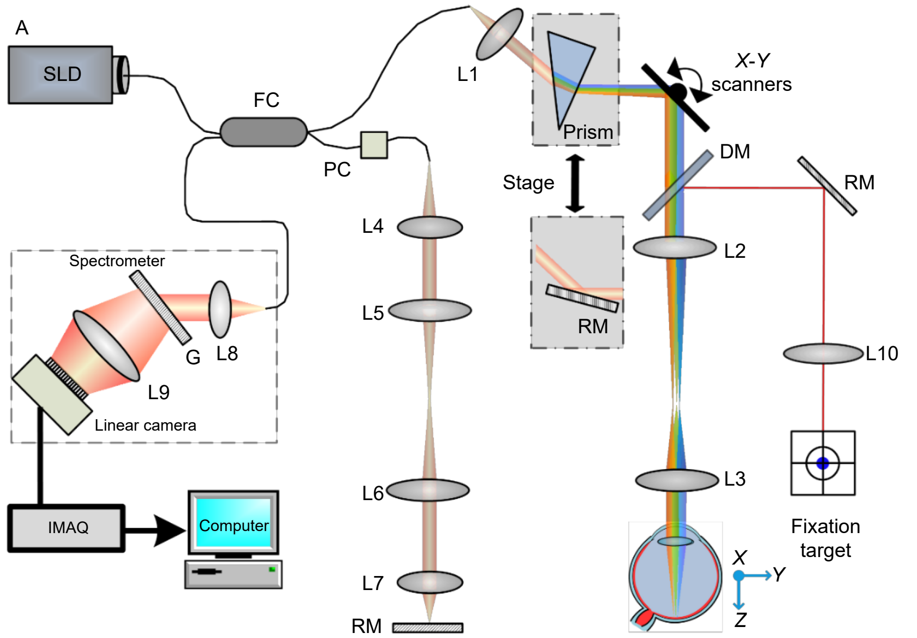

Fig. S6 | Schematics of 850 nm OCTA system for retinal imaging with SELF and point configuration. SLD: superluminescent diode source; FC: fiber coupler; PC: polarization controller; L1–8 & L10: achromatic lenses; L9: camera lens; RM: reflective mirror; G: transmission grating; IMAQ: image acquisition card.

doublets (AC508-200-B; L2) and two sets of 75 mm doublets (AC508-075-B; L3).

The spectrometer is comprised of a customized collimating lens L8, a transmission grating (PING-1765-025, Ibsen Photonics), a home-made multi-element camera lens and a line scan camera with pixel size of 10 μm × 200 μm (width × height) (Octoplus, EV71Y01CCL2210-BB3). The overall spectrometer efficiency was measured to be approximately 0.7. We used all 2048 camera pixels for detection and the measured total ranging depth is 4.1 mm in air. The 6 dB intensity ranging depth was measured to be 2.83 mm in air (Fig. S6).

In Fig. 3(g–j), the full spectral bandwidth of the light source is employed. The total ranging depth of the system was measured to be 4.2 mm in air and 6 dB ranging depth range was ~2.2 mm in air. In the sample arm, a prism (BK7) with apex angle of 33° is used to generate the line field, which is simulated to be ~81 μm at the retina with the Zemax model, assuming the eye focal length of 17.2 μm. We split the full spectrum line field length using M = 9 Hamming windows with size of 1400 pixels and spacing of 416 pixels. Transverse spacing r between two adjacent spectral bands at the retina is calibrated to be ~8.7 μm using a USAF 1951 resolution chart. With the spectral window, the partial spectrum axial resolution is 9.83 μm in air, corresponding to 7.12 μm in retina with refractive index = 1.38.

2.2 Maximum permissible exposure of line field

The intensity profile of the line field was estimated using the light source spectrum captured by the spectrometer (Fig. S7(a)). The transverse positions of spectral bands were calibrated using a USAF 1951 resolution chart. According to the Eq. (1), the angular subtense in Y-axis (α_Y) obtained using 'Most restrictive ratio' analysis is shown in Fig. S7. The extended source correction factor is C_E. Note that maximum exposure power limit calculated using C_E applies only to the partial power within the angular subtense δ, instead of the total power. As shown inFig. S7, there is some power that falls outside the angular subtense δ. Therefore, assuming the optical power incident on the cornea is a for point scanning configuration and the power outside of the angular subtense is b, The corresponding power for the SELF configuration is calculated as $(a \times C_E) / (1 - b)$.

For all the experiments conducted with the 850 nm system except for Fig. 3(g–j), the optical power incident on the cornea is 0.84 mW for the point-scanning configuration. The extended source correction factor C_E is (5.372 mrad +1.5 mrad) / (1.5 × 2 mrad) = 2.29 (Fig. S7(a, b)). The corresponding calculated power for the SELF configuration is larger than 0.84 mW × 2.29 = 1.924 mW.

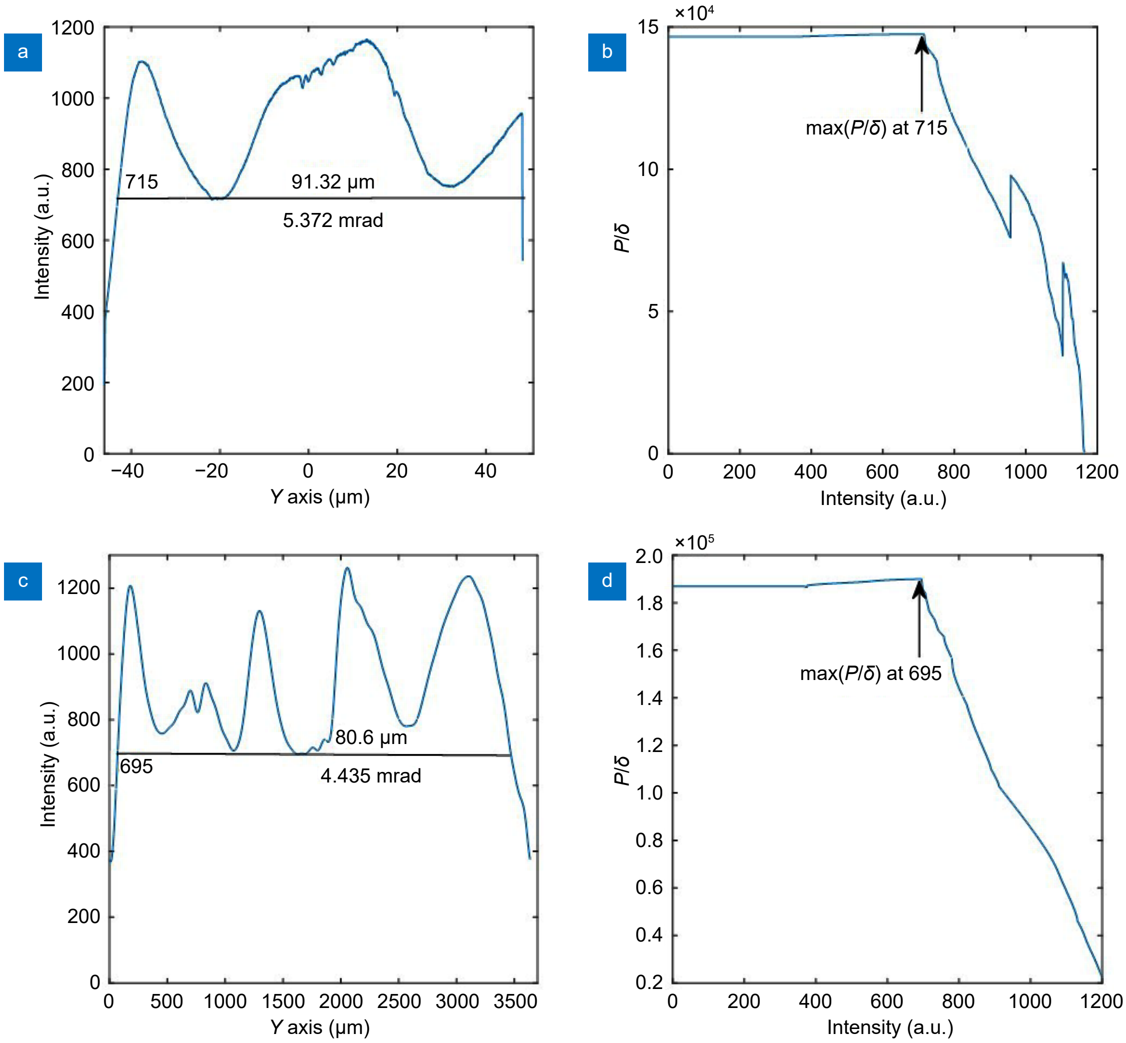

Fig. S7 | Maximum permissible exposure characterization for 850 nm system. (**a**, **b**) System with 90 nm spectral bandwidth: (a) Intensity profile of focus along *Y*-axis of 850 nm SELF-OCT system with spectral bandwidth ranging from 805 nm to 895 nm; (b) Corresponding ratio between partial power (*P*) within window width (*δ*) for 'Most restrictive ratio' method. The window width is 91.32 μm (5.372 mrad) when the ratio reaches the maximum. (**c**, **d**) System with 175 nm spectral bandwidth: (c) Intensity profile of focus along *Y*-axis of 850 nm SELF-OCT system with spectral bandwidth ranging from 755 nm to 930 nm; (d) Corresponding ratio between partial power (*P*) within window width (*δ*) for 'Most restrictive ratio' method. The window width is 80.6 μm (4.435 mrad) when the ratio reaches the maximum.

For Fig. 3(g–j) where the 175 nm full spectral bandwidth from 755 nm to 930 nm is used, the optical power incident on the cornea is ~1.2 mW for the point-scanning configuration. The extended source correction factor C_E is (4.435 mrad +1.5 mrad) / (1.5×2 mrad) = 1.9783 (Fig. S7(c, d)). The corresponding calculated power for the SELF configuration is larger than 1.2 mW × 1.978 = 2.374 mW.

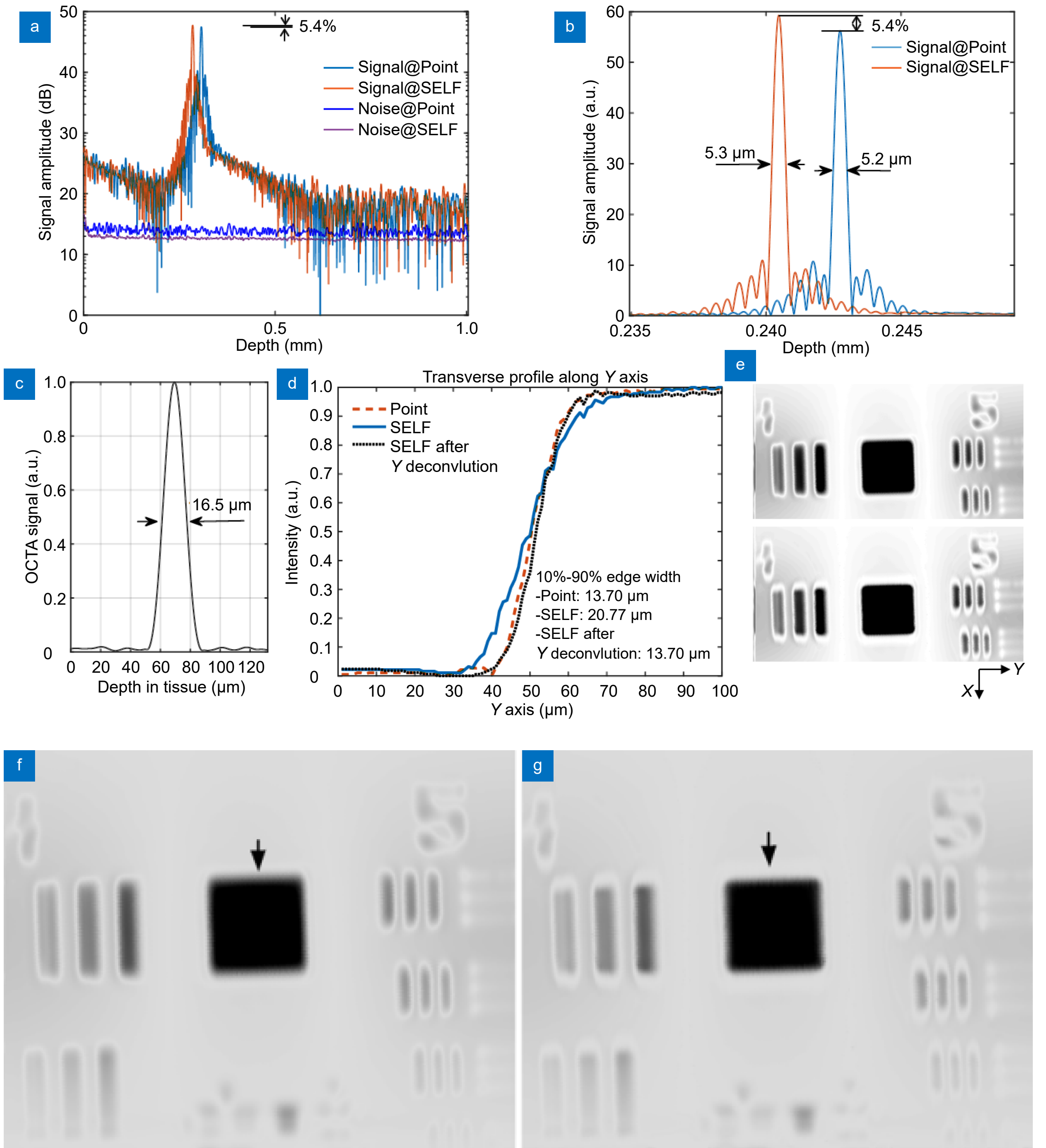

Fig. S8 | Sensitivity and spatial resolution characterization of the 850 nm system. (**a**) Axial profiles and noise floor of full-spectrum fringe data in log scale. (**b**) Axial profiles of full-spectrum fringe data in linear scale with FWHM axial resolution being 5.2 μm and 5.3 μm, respectively. (**c**) Normalized axial profile of a partial-spectrum fringe data (4th partial spectrum). (**d**) Transverse profile along *Y*-axis of a quasi-monochromatic beam (orange dashed line), beam of the 4th partial spectral band before (blue solid line) and after *Y*-deconvolution (black dot line). (**e**, upper panel) the image of USAF 1951 resolution chart obtained using the partial-spectrum of the 4th spectral band before *Y*-deconvolution, magnified view is shown in (**f**). (**e**, lower panel) The image of USAF 1951 resolution chart obtained using the partial-spectrum of the 4th spectral band after *Y*-deconvolution, magnified view is shown in (**g**). Arrow indicates *Y* direction in (f, g).

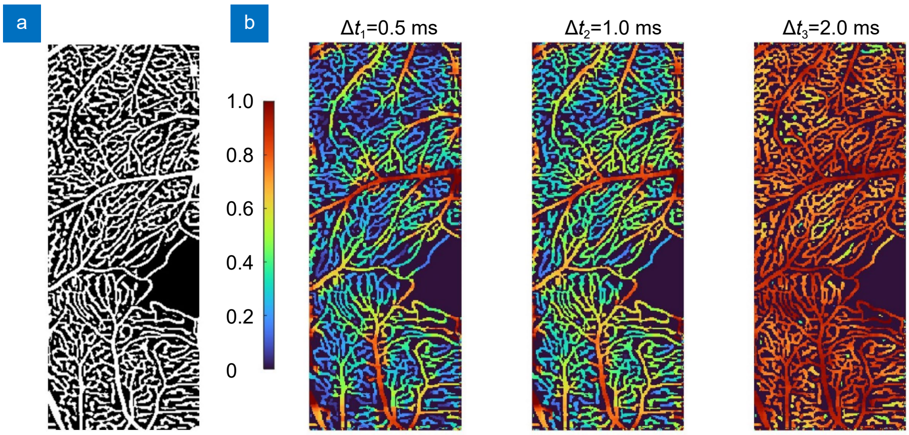

Fig. S9 | En face projections of normalized retinal angiograms. (**a**) Vessel mask. (**b**) Normalized and color-coded retinal angiograms with different interscan time intervals.

References

S1. Yun SH, Tearney GJ, Bouma BE et al. High-speed spectral-domain optical coherence tomography at 1.3 μm wavelength. *Opt Express* **11**, 3598–3604 (2003).

S2. Leitgeb R, Hitzenberger CK, Fercher AF. Performance of fourier domain vs. time domain optical coherence tomography. *Opt. Express* **11**, 889–894 (2003).

S3. Schulmeister K, Gilber R, Seiser B et al. Retinal thermal laser damage thresholds for different beam profiles and scanned exposure. *Proc SPIE* **6844**, 68441L (2008).

S4. International Electrotechnical Commission. Safety of laser products - Part 1: equipment classification and requirements. IEC 60825–1: 2014.